RESEARCH PAPER

PCCP
www.rsc.org/pccp

Angle resolved ion scattering spectroscopy reveals the local topography around atoms in a liquid surface

Gunther Andersson,* Thomas Krebs and Harald Morgner

Wilhelm-Ostwald-Institute for Physical and Theoretical Chemistry Leipzig University, Linnestr. 3, 04103 Leipzig, Germany. E-mail: G.Andersson@rz.uni-leipzig.de; Fax: +49-341-9736090

Received 28th April 2005, Accepted 14th June 2005
First published as an Advance Article on the web 6th July 2005

Neutral impact collision ion scattering spectroscopy under normal incidence is known to yield the concentration depth profiles of all elements except hydrogen at the surface of liquids and other amorphous material. In the evaluation of the data one tactically has to assume that the top surface layer and the adjacent layers are laterally homogeneous. In the present paper we establish that the angular resolved mode of this spectroscopy is able to test with high accuracy whether the lateral homogeneity is valid and—if this is not the case—in which way the top layer is structured. In particular, it is possible to map out the local environment of selected atoms. We expect that this so far inaccessible information on the local topography at liquid surfaces will have an impact on the understanding of reactions at the gas/liquid interface.

Introduction

The molecular structure of liquid surfaces is of interest in many fields like biochemistry, atmospheric research and in a great variety of technical applications. Recently the question which has attracted attention is where the alkali ions are positioned in a liquid surface.[1,2] Commonly liquid surfaces are investigated by measuring the surface tension. Information about the structure of the surface is derived indirectly by determining the surface excess or the surface coverage from adsorption isotherms. In the past decades several methods have been developed to investigate directly the molecular structure of liquid surfaces. With neutron reflectivity (NR) the surface composition can be measured directly.[3,4] X-Ray reflectivity reveals the electron density profile at a liquid surface and is used to determine the roughness of interfaces.[5,6] In favourable cases the electron density profile can be interpreted in terms of the profile of chemical species.[7] With non-linear optical methods the orientation of molecules is determined.[8–10] Angle resolved photoelectron spectroscopy has been used to determine concentration depth profiles.[11,12] In the evaluation of the measurements of all these methods the molecular structure of the surface has to be treated as laterally homogeneous. Thus using these methods the lateral molecular structure is not subject of the research.

The present paper is focused on the lateral molecular structure of liquid surfaces. This is of fundamental interest and has also applications for the interaction of liquid surfaces with their environment. One example is the uptake of gas molecules. Besides the composition[13–15] the topography of a surface might be important for this process as a preceding step of reactions at the gas/liquid interface. Techniques to explore the lateral structure of a solid surface like the scanning tunneling microscope (STM) or the atomic force microscope (AFM) cannot be used for liquid surfaces due to the rapid motion of the molecules. The only experimental method known to us for determining relative positions of atoms in a liquid surface is extended X-ray absorption fine structure (EXAFS), which was used to determine the radial distribution of matter around bromide.[16]

Neutral impact collision ion scattering spectra (NICISS) is used in our group to determine concentration depth profiles of the elements.[17–19] Up to now we have tacitly assumed for the evaluation of the data, that the top surface layer and the adjacent layers are laterally homogeneous. Here we show that the angular mode of NICISS (ARISS) can be used to reveal the local topography around atoms in a liquid surface, and so to gain information about the lateral molecular structure of a liquid surface. The impact collision ion scattering spectra (ICISS) at grazing incidence were used previously to determine the lattice structure of single crystal solid surfaces.[20,21]

In computer simulations the density profiles, diffusion constants, surface tension, orientation of molecules or concentration depth profiles, which treat the surface as laterally homogeneous, are determined.[1,2,22] From pair correlation functions the distances of molecules relative to each other are determined. Undoubtedly it should be possible to determine parameters which describe the topography of the surface, but this has not been done yet.

The importance of the topography of liquid surfaces can be illustrated by the difference in the reaction rate of metastable helium atoms with halide ions, which is used for spectroscopic purposes[23] and which is one type of gas/surface reactions. Surfaces of formamide solutions of the surfactants tetrabutylammonium iodide (Bu_4NI) and tetrabutylammonium bromide (Bu_4NBr) show a difference in the reaction rate of about a factor of 9 between iodide and bromide,[24] while the surface excess differs only by a factor of 2.[17] The reason might be a difference in the local topography around both ions caused by the difference in the interaction energy with their next neighbors. It is known that the solvation enthalpy of ions both in formamide and water becomes less negative and that the lattice enthalpy of alkali halides decreases[30] with increasing size of the ions. This means that the attractive interaction between ions and solvent molecules or counter ions is greater for ions with a small ionic radius than for those with a greater radius. As a consequence the tendency for iodide to be surrounded with other molecules in the surface is less than for bromide. Thus it can be expected that the topography around iodide has a more open structure than that around bromide.

DOI: 10.1039/b505965h

Experimental

We determine the topography in the vicinity of an atom in a liquid surface by measuring NICIS spectra at different polar angles. NICISS uses the inelastic loss of energy of projectiles with a kinetic energy of some keV to determine concentration depth profiles of elements at liquid surfaces with a depth resolution of some ångströms.[17–19] Projectiles moving through matter lose energy due to the low angle scattering and electronic excitations (stopping power). The energy loss can be converted into depth information. Up to now our experiments were carried out at an angle of incidence close to the surface normal. At this geometry we can determine only structures perpendicular to the surface and thus the spectra were interpreted by assuming a laterally homogeneous surface structure. The procedure to determine concentration depth profiles from the NICIS spectra is described in detail in ref. 19.

The surfaces investigated are that of 0.25 molal solutions of tetrabutylammonium iodide (Bu_4NI), tetrabutylphosphonium bromide (Bu_4PBr) and tetrabutylammonium bromide (Bu_4NBr) and 0.35 molal solutions of potassium iodide (KI) in formamide. Formamide was purchased from Aldrich, Bu_4NI, Bu_4PBr and Bu_4NBr from Merck and KI from Fluka. The substances were used without further purification.

In order to gauge the zero mark of the depth scale we carried out NICISS measurements at a gas jet of the substances CH_2I_2, $CHBr_3$ and $P(CH)_3$. The density in the gas phase was kept so low, that the only interaction projectiles encounter with another atom is during the back scattering process. Thus the gas phase spectra show a spectrum which represents the projectile being back scattered from the outermost layer. The width of the spectrum is due to the distribution of inelastic energy losses during back scattering.

Results

Criterion for the lateral homogeneity of the topography

As a first example we consider the surface of the solvent formamide probed with ARISS. The energy loss spectra of oxygen derived from the measurement as described in detail in ref. 19 are the same at different polar angles as shown in Fig. 1. The spectra can be fitted with a single depth profile[25] taking into account the energy resolution of the method and the relation between the depth scale and the energy loss scale as function of the angle of incidence of the projectiles.

The relation between the energy loss and the depth at a fixed polar angle is calculated with the algorithm:

$$
\begin{aligned}
E_i^{\text{in}} &= E_{i-1}^{\text{in}} - \frac{\Delta d}{\cos(\theta + 12^\circ)} \mathrm{Sp}\left(E_{i-1}^{\text{in}}\right) \quad \text{with } i = 1 \text{ to } n \\
E_0^{\text{in}} &= E_0 \\
d &= n\,\Delta d \\
E_0^{\text{in}} &= k_1\, E_n^{\text{in}} - Q_{\text{in}} \\
E_j^{\text{out}} &= E_{j-1}^{\text{out}} - \frac{\Delta d}{\cos(\theta)} \mathrm{Sp}\left(E_{j-1}^{\text{out}}\right) \quad \text{with } j = 1 \text{ to } n
\end{aligned}
\tag{1}
$$

where E_0: primary energy of the projectile; E_i^{in}: energy of the projectile after passing the i-th layer on the way into the bulk; Δd: thickness of the n layer; d: depth; E_0^{out}: energy of the projectile after back scattering; k: kinematic factor of the energy loss during back scattering; E_j^{out}: energy of the projectile after passing the j-th layer on the way back to the surface; Sp: stopping power, the energy dependence of the stopping power was taken into account; θ: polar angle, *i.e.* angle between the surface normal and the direction to the detector, where $78^\circ - \theta$ is the angle between the direction of the impinging ions and the surface, the angle of incidence.

The depth profile of oxygen is found to be a step profile with the onset at the outermost layer. This is in agreement with the finding, that formamide molecules are lying flat on the surface.[26,27] As a second example the ARIS spectra of benzyl alcohol can also be fitted with a single depth profile for all angles.[25] Different to formamide the depth profile of oxygen is not constant but shows a depletion at the surface and an enrichment at a depth of about 5 Å. The enrichment in a deeper layer is due to the orientation of the molecules at the surface.[22] Thus, the evaluation of ARISS data allows to test whether the assumption of lateral homogeneity of the topography of the surface is justified, irrespective of whether the corresponding depth profile is constant or not. The concept "lateral homogeneous topography" means that there is no correlation between the position of an element or a subunit of a molecule or a molecule and the topography in its local environment.

The same test on the lateral homogeneity turns out to be negative if it is applied to iodide in the solution of Bu_4NI in formamide. The energy loss spectra of the iodide of the 0.25 molal solution of the ionic surfactant Bu_4NI are shown in Fig. 2. The zero mark of the energy loss scale is gauged with the gas

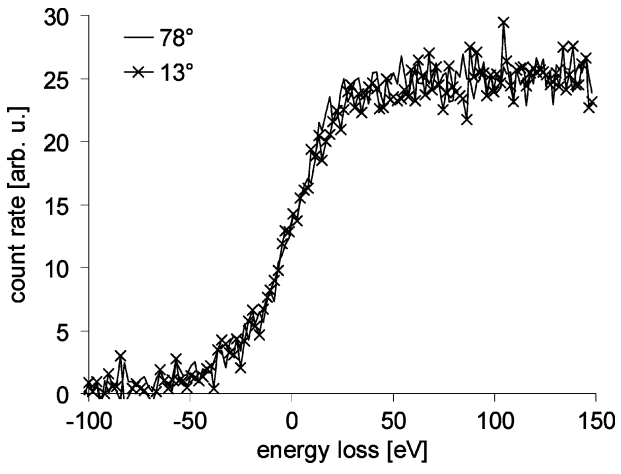

Fig. 1 Energy loss spectra of oxygen of pure formamide at an angle of incidence close to the surface normal (78°) and at grazing incidence (13°).

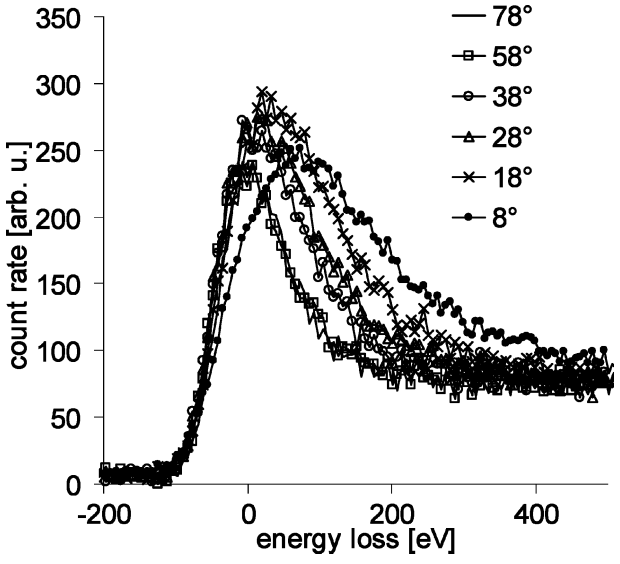

Fig. 2 Energy loss spectra of iodide of a 0.25 molal Bu_4NI solution in formamide.

phase spectra.[28] The iodide has an enrichment in the outermost layer, which is due to the surface active cation Bu_4N^+. We find a shift of the maximum to a greater energy loss with decreasing angle and a broadening of the structure. A peak appearing in the outermost layer at an angle of incidence close to the surface normal cannot be shifted to a greater energy loss at grazing incidence assuming only a single depth profile. Thus the test on lateral homogeneity fails in this case. The only possible explanation for the shift of the maximum is, that the iodide is located in a valley-like structure. The projectiles impinging on the surface close to the surface normal see an uncovered iodide while projectiles impinging at grazing incidence have to pass matter—the adjacent hills—before hitting the iodide in the outermost layer.

The examples show the criterion for the classification of the topography. The spectra that can be fitted with a single depth profile for all angles of incidence indicate a lateral homogeneous topography, which means that the surface is flat. The other spectra indicate a lateral inhomogeneous topography in the vicinity of the considered atom.

The test on the lateral homogeneity turns out to be negative also for the spectra of bromide and phosphorus of the 0.25 molal solutions of Bu_4NBr and Bu_4PBr and iodide of the 0.35 molal solution of KI in formamide.

Determining the spectra of the outermost layer

In order to determine quantitative parameters describing the topography in the vicinity of an atom we have to determine the spectra of solely the outermost layer at the different angles of incidence. For this purpose we divide the surface near region into three parts as sketched in Fig. 3: bulk, outermost layer and top layer. It may be assumed that species in the bulk have lateral positions, which have no correlation with the structure of the surface. The spectrum of the atoms in the bulk corrected for the angle of incidence is independent of this angle since there is no correlation between the lateral position of these atoms and the structure of the top layer, *i.e.* we average over the influence of the top layer structure on the bulk spectrum. The surface is divided into the atoms of the considered element in the outermost layer, *i.e.* those atoms which are not covered by matter, and the matter around these atoms, the top layer, which determines the topography around an atom in the surface. The atoms of the outermost layer appear at top view at the same position as the gas phase spectrum of the specific element.[28] Thus in a spectrum at top view, *i.e.* an angle of observation close to the surface normal (78°), the energy loss spectrum is divided into the spectrum of the outermost layer, which is represented by the gas phase spectrum, and the bulk contribution, which is the total energy loss spectrum minus the gas phase spectrum. This is shown for iodide of Bu_4NI in Fig. 4. The ratio between the gas phase spectrum and the spectrum of the liquid phase is chosen so that the contribution of the outermost layer is as great as possible but that the remaining bulk spectrum does not go negative. With this procedure we assign all atoms which do not belong to the outermost layer to the bulk contribution. In Fig. 4 it can be seen, that in the depth profile of the bulk contribution of iodide the concentration at a depth of about 6 to 12 Å is significant greater than the bulk concentration. This part of the depth profile might be comparable with the diffusive layer in the electrical double layer model of the Stern model.[29] From the area of the spectrum of the outermost layer at an angle of observation of 78° the number of atoms in the outermost layer can be determined, which is in this case $(6.4 \pm 0.5) \cdot 10^{13}$ atoms cm^{-2}. Since the spectrum of the bulk is independent of the angle of observation, the bulk contribution is subtracted from the spectra measured at the other polar angles taking into account the relation between the energy loss scale and depth scale at a given polar angle.

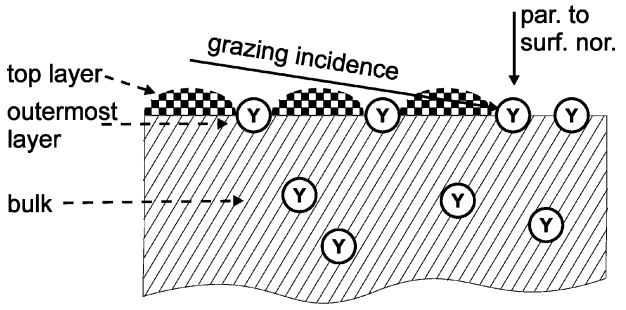

Fig. 3 The surface near region of the target is divided into bulk, outermost layer and top layer. The trajectories of projectiles are sketched, which impinge on the surface parallel to the surface normal or at grazing incidence.

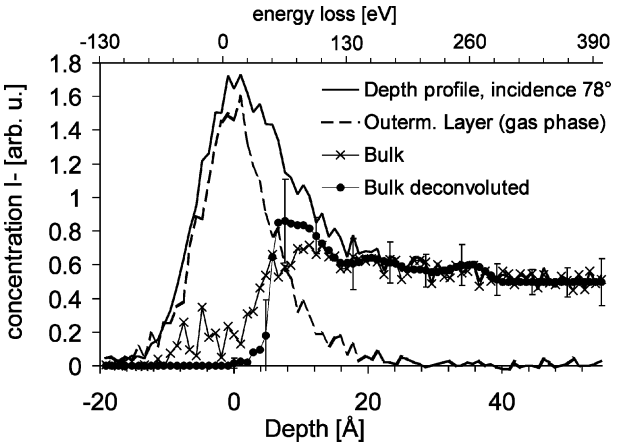

Fig. 4 Depth profile and energy loss spectrum of iodide (Bu_4NI) at an angle of incidence of 78° with the separation into the contribution of the outermost layer and the bulk. The error bars of the deconvoluted bulk profile are calculated from the statistics of the genetic algorithm.

Before we subtract the spectrum of the bulk we first have to take into account the influence of the energy resolution of the method on the slope of the spectra. The width of a gas phase spectrum is mainly determined by the distribution of the inelastic loss of energy during the back scattering process but also by the energy spread of the ion beam and the time length of a single bunch of the pulsed ion beam. Each spectrum of an element is a convolution of the distribution of the inelastic loss of energy with the depth profile of the specific element, which is in the case of a gas phase spectrum a delta function. The relation between the width of the distribution of the inelastic loss of energy and the slope of the concentration depth profile of the bulk contribution is different for all angles of observation. Thus the spectrum of the bulk contribution determined at an angle of observation of 78° has to be corrected for the inelastic loss of energy during the back scattering process before it is converted to the depth scale at another angle of observation. The correction is carried out by a deconvolution with the gas phase spectrum of the specific element. The converted depth profile is then convoluted again with the gas phase spectrum. The deconvoluted bulk spectrum is shown in Fig. 4. The deconvolution is carried out with the genetic algorithm as described in ref. 17. In Fig. 5 we show the separation of the spectra of bromide and phosphorus of the Bu_4PBr solution into the outermost layer and the bulk contribution. The maximum of the bromine is shifted a little to a greater depth. The number of bromine ions in the outermost layer is $(4.7 \pm 0.5) \times 10^{13}$ atoms cm^{-2}. This is smaller than the number of the phosphorus atoms which is $(6.3 \pm 0.5) \times 10^{13}$ atoms cm^{-2}.

In Fig. 6 the separation into the spectrum of the outermost layer and that of the bulk is shown for an angle of observation

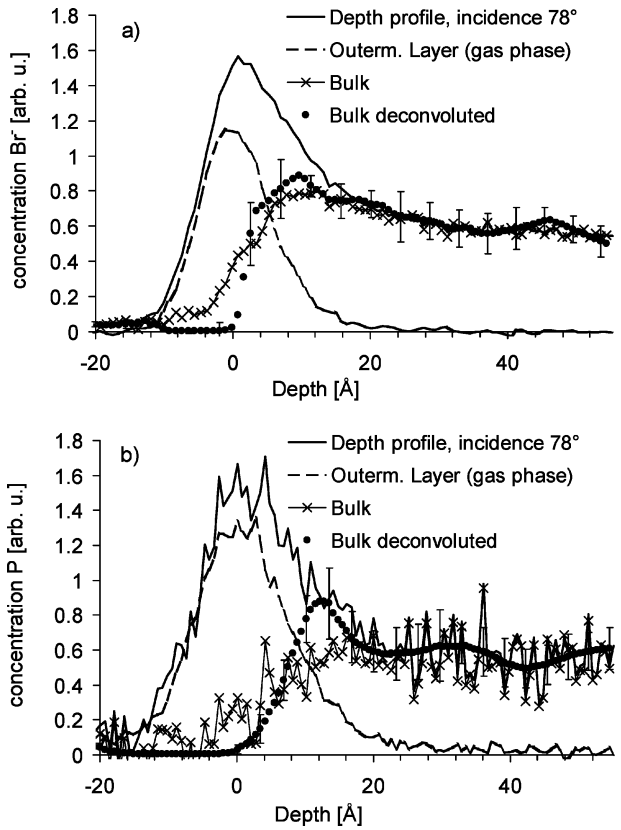

Fig. 5 Depth profile of bromide and phosphorus (Bu_4PBr) at an angle of incidence of 78° with the separation into the contribution of the outermost layer and the bulk. The error bars of the deconvoluted bulk profiles are calculated from the statistics of the genetic algorithm.

of 28°. It should be noticed that the relationship between the depth scale and the energy loss scale is different than in Fig. 4. Both the deconvoluted and the convoluted spectra of the bulk determined from the spectrum at 78°are shown. The convoluted spectrum is subtracted from the total iodide spectrum obtained at 28° resulting in the spectrum of the outermost layer at 28°. Carrying out this procedure for all angle of observation <78° we obtain the spectrum of the outermost layer of the

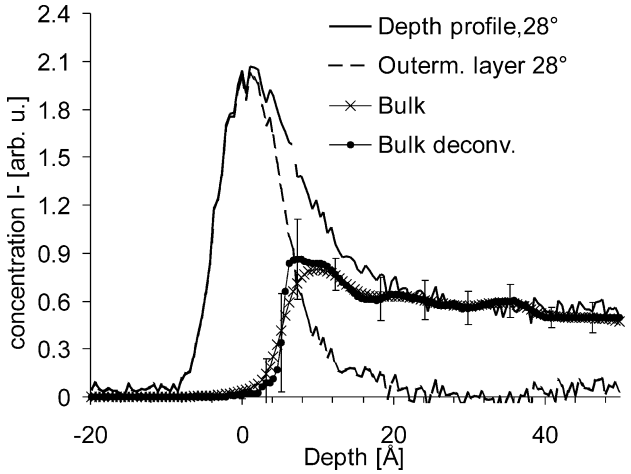

Fig. 6 Depth profile and energy loss spectrum of iodide (Bu_4NI) at an angle of incidence of 28° with the separation into the contribution of the outermost layer and the bulk. The bulk contribution at 28° is obtained from that of 78°, which was deconvoluted with the gas phase spectrum, converted from the energy loss scale of 78° to that of 28° and finally convoluted with the gas phase spectrum. The relation between the width of the distribution of the inelastic loss of energy and the slope of the concentration depth profile of the bulk contribution is different for all angles of observation.

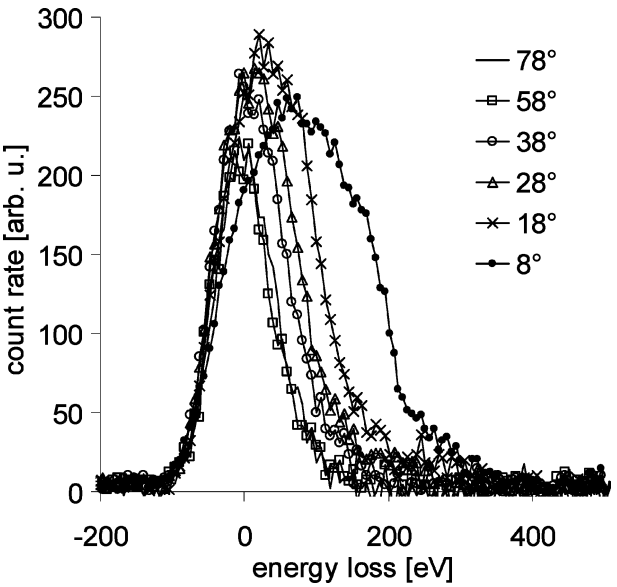

Fig. 7 Energy loss spectra of iodide (Bu_4NI) of the outermost layer at different angles of incidence. They are the difference between the spectra shown in Fig. 2 and the contribution of the bulk.

considered element for different polar angles, which is shown for the anion iodide of Bu_4NI in Fig. 7. The top layer becomes visible in the change of the spectra of the outermost layer with the angle of incidence. The quantitative description of the top layer is gained with the fitting procedure described below.

The sketch of the surface in Fig. 3 seems to imply that the local topography around an atom is the same for all atoms of a specific element. This feature of the sketch is only due to practical reasons for the drawing of the figure. Due to the low degree of long range order in a liquid surface there will be a great variety of different configurations. It must be emphasized here that our method averages over all different possibilities that occur in a liquid surface and that the method itself does not require the existence of a long range ordered surface.

Parameter describing the local topography

The spectra of the outermost layer at different polar angles are fitted by convoluting the gas phase spectrum with the distribution of the probabilities, that a projectile encounters a certain energy loss in the top layer. The convolution is carried out as a discrete sum and is given by

$$I(E,\theta) = \sum_i I(E - \Delta E_i, \text{gas phase}) f(\Delta E_i) \qquad (2)$$

where $I(E,\varphi)$ is the spectrum of the outermost layer at the angle φ, $I(E - \Delta E_i$, gas phase) is the gas phase spectrum shifted about ΔE_i and weighted with the factors $f(\Delta E_i)$, which are the fitted values. For 78° $f(\Delta E_i = 0) = 1$ and $f(\Delta E_i > 0) = 0$. The distribution of the probabilities are the fitting parameters. This fitting procedure in effect examines what is the probability at a fixed polar angle that the projectiles encounter on their way to the target atom and back a certain amount of matter. Due to the rapid motion of the molecules in the liquid the distribution of the probabilities will be a broad distribution and will not have well separated peaks. It must be emphasized here that for a single projectile the target appears frozen, since the time the ion is in contact with the target is much shorter than the typical time scale of the molecular motion, but each projectile will encounter a different configuration.

The distribution of the probabilities for the energy loss for iodide of Bu_4NI are shown in Fig. 8. The ΔE_i are chosen so that the intervals of the depth scale, which is the path length of the projectiles in the matter corrected by the angle of incidence, are

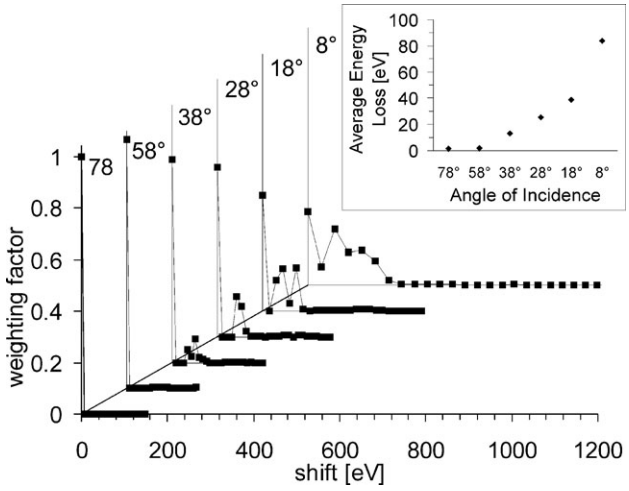

Fig. 8 Weighting factors $f(\Delta E_i)$ for the convolution of the spectra of the outermost layer of iodide (Bu_4NI) at different angles of incidence.

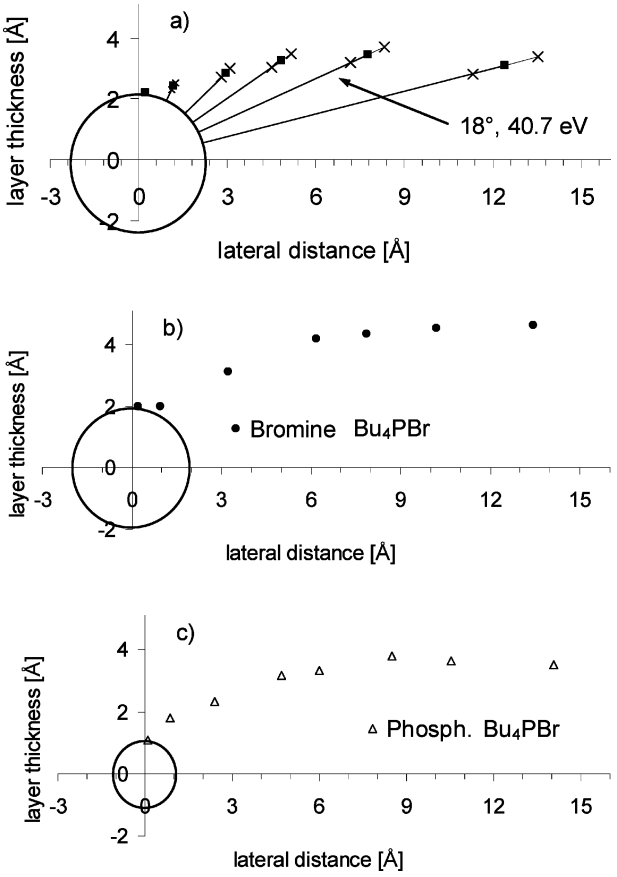

Fig. 9 The energy loss at different angles of observation converted into the depth information: (a) iodide of the 0.25 molal Bu_4NI solution, (b) bromide of the Bu_4PBr solution, (c) phosphorus of the Bu_4PBr solution. The results for bromine of Bu_4NBr are the same as that of Bu_4PBr and are not shown here. The top layer around iodide of Bu_4NI has a height of about 3.3 Å and that around bromine of about 4.6 Å. In the direction close to the surface normal (78°) the target atoms are not covered in all cases and directly accessible for the projectiles. Representatively, we show the errors in (a). The crosses mark the error of the length of the lines, which is the error of the amount of matter in the specific direction. The error takes into account the uncertainty of the difference in the TOF distance for the spectra of the liquid and the gas phase, the uncertainty in the height of the gas phase spectrum with respect to that of the liquid, the uncertainty in the fitting procedure and the possible influence of the gas phase above the surface.

equal for all angles. We see that the probability for a projectile to directly hit an iodide ($f(\Delta E_i = 0)$) decreases with decreasing angle of incidence. At the same time the $f(\Delta E_i > 0)$ increase. The distribution of the $f(\Delta E_i > 0)$ seems to bear a structure, but its interpretation would require more experience with other systems. The weighted average energy loss $\overline{\Delta E}$ is calculated from the weighting factors $f(\Delta E_i)$ by

$$\overline{\Delta E} = \frac{\sum_i \Delta E_i f(\Delta E_i)}{\sum_i f(\Delta E_i)} = \overline{\Delta d}\,\mathrm{Sp} \qquad (3)$$

where $\overline{\Delta d}$ is the average amount of matter as the path length that the projectiles have to pass before they hit the specific atom in the outermost layer and Sp is the stopping power. The energy dependence of the stopping power was taken into account. The weighted average energy loss is shown as function of the polar angle as an inset in Fig. 8. Taking into account the energy loss per unit layer thickness we obtain the average amount of matter around the iodide as pass length of the projectile, the $\overline{\Delta d}$.

Discussion

In order to obtain the structure of the top layer and thus a picture of the topography we draw in a diagram a line with a length corresponding to the amount of matter detected in the top layer. This is shown for iodide in Fig. 9a. The starting point is on the outer shell of the target atom and the direction is given by the polar angle. For the radius of the outer shell we choose the ionic radius of iodide. The end points are marked with solid squares. The crosses mark the error of the length of the lines, which is the error of the amount of matter in the specific direction. At 78° the end points coincide with the outer shell of the target atom which means that the target atom is uncovered in this direction and directly accessible for the projectiles. The envelope of the end points of the lines shows the distribution of the average amount of matter around the considered atom. We want to emphasize here, that the envelope is an average over all azimuthal angles, which is due to the motion of the molecules. A specific direction cannot be selected which is due to the long range rotational symmetry of a liquid surface.

The envelopes of the topography around bromide and phosphorus of Bu_4PBr are shown in Fig. 9b and c. For the radius of the outer shell we choose the ionic radius of bromide and the covalent radius of phosphorus. The energy loss spectra of bromide with Bu_4P^+ and Bu_4N^+ (not shown here) as cations are the same within the statistical error. Thus the topography around bromide is the same for both cations. Comparing the anions iodide and bromide of Bu_4XY (X: N or P, Y: I or Br) we find as a common feature that both ions are located in a valley-like structure. This finding corresponds to the fact that both ions are not surface active by themselves. Their excess at the surface is caused by the surface activity of the Bu_4X^+ cations and the demand of charge equilibrium. The orientation of the Bu_4P^+ cation, which can be concluded from the local environment of the phosphorus, corresponds to that which was proposed already by Eschen *et al.*:[11] three of the butyl chains are laying on the surface while the fourth points into the bulk.

In Fig. 10a we compare the topography around iodide and bromide in the surface of the surfactant solution. For the comparison we choose a plot in such a way that the envelopes characterizing the local environment of both species are on the same height at a lateral distance where the layer thickness saturates. At this distance the average layer thickness around the species should be met, which is composed mainly by the butyl chains of the cations. The bromide and the envelope showing the topography around the ion have to be shifted about −1.1 Å parallel to the surface normal in order to be on the same height as the envelope of iodide at a lateral distance where the layer thickness saturates. This means that the bromide is located deeper in the bulk than the iodide. We do

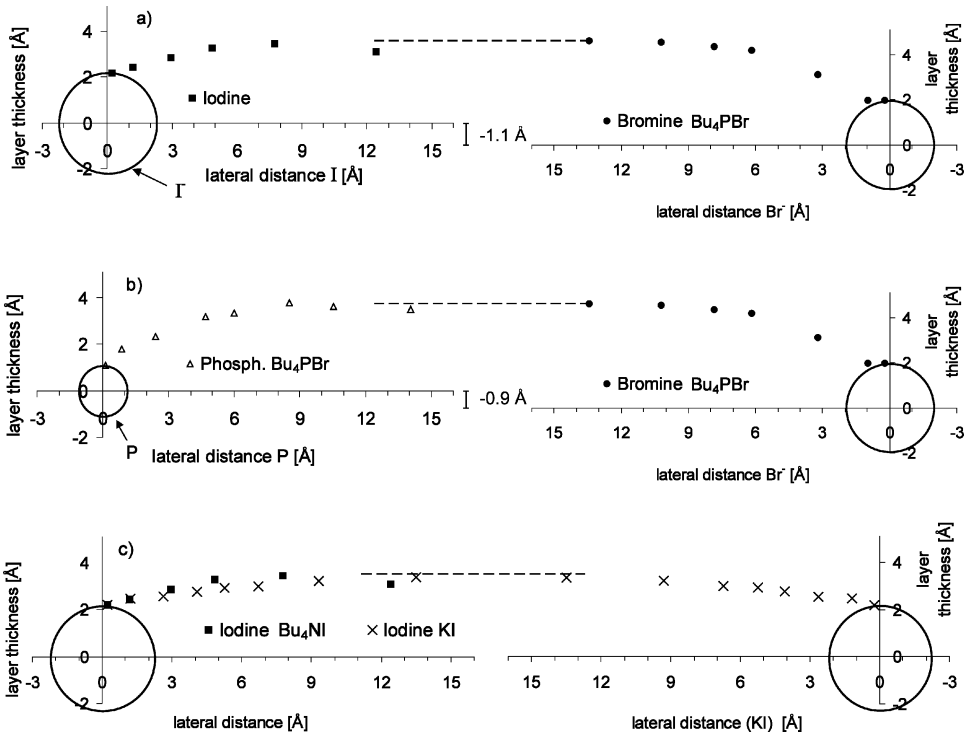

Fig. 10 (a) Comparison of the topography around iodide and bromide of the compounds Bu_4NI and Bu_4PBr, (b) comparison of the topography around phosphorus and bromide of the compound Bu_4PBr, (c) comparison of the topography around iodide of the compounds KI and Bu_4NI. For the comparison we choose a plot in such a way that the layer thickness in the local environment of both species are on the same height at a distance where the layer thickness saturates. In (a) the bromide is shifted about −1.1 Å parallel to the surface normal and in (b) about −0.9 Å.

not intend to draw with the graph a picture of the topography between both halide ions for the case they would be in the same surface. This is not possible since no special direction in a liquid surface can be selected. The intention is only to show the difference in the topography around both ions. The difference in the local environment is reflected also in the fraction of the anions that can be assigned to the outermost layer as can be seen in Fig. 4 and Fig. 5a. The fraction of iodide in the outermost layer is greater than that of bromide.

The difference in the topography between both halide ions can be explained considering the difference in their ionic radii. Because of the high coverage of the solutions with surfactant molecules and the finding, that the environment of the iodide is isotropic, it is assumed that the ions form two-dimensional clusters of anions and cations in the surface.[23] The iodide with the greater ionic radius has the less negative solvation enthalpy and lower lattice enthalpy.[30] Thus we expect that iodide is bounded less strongly to the adjacent molecules in the surface than bromide, which causes the more open structure around iodide. The difference in the topography also explains the low reaction rate of metastable helium atoms with bromide compared to iodide.[24]

We compare the topography of bromide and phosphorus in Fig. 10b. The figure is composed similar to Fig. 10a. The bromide is shifted about −0.9 Å parallel to the surface normal. Bromide and Bu_4P^+ will form in the same way as Bu_4NI two-dimensional cluster. Thus the environment of both bromide and phosphorus will consist of the butyl chains. The difference in the local environment of both species is reflected also in the fraction of ions that can be assigned to the outermost layer as can be seen in Figs. 5a and b. The fraction of anions to cations in the outermost layer is about 0.75. This is due to the fact that the cation is the surface active species.

We compare in Fig. 10c the topography around iodide for both iodide compounds KI and Bu_4NI. The figure is composed similar to Fig. 10a. For comparison of the slope of the envelopes the topography around iodide of KI is shown also on the right side. The envelopes of iodide saturates at the same height in both cases. There is only a small but significant difference in the slope at a lateral distance between 3 and 9 Å. In this range the layer around the iodide in the KI solution is less thick than that in the Bu_4NI solution. The similarity is surprisingly since the composition around the iodide is different in both cases. In the first case iodide will be present at the surface as a solvated ion and not in two-dimensional clusters as in the latter case[23] and the surface coverage with iodide in the case of KI is much less than in the case of the surfactant Bu_4NI. The tendency to form a more open structure in the case of KI as found in the small difference at a lateral distance between 3 and 9 Å might be due to the smaller size of the solvent molecules compared to that of the Bu_4N^+ cations. An independent proof of this finding will be the comparison of metastable induced electron spectra (MIES) of KI and Bu_4NI solutions.

The relative position of the cation and anion in the direction parallel to the surface normal has consequences for the surface potential. Shifting the anion towards the bulk with respect to the cation will make the surface potential more negative. The position of the bromide is deeper in the bulk than that of iodide. Thus it can be expected that the surface potential of the bromide salts is more negative than that of the iodide, which is found in the measurements of the surface potential.[31]

Finally we want to discuss other possible sources than the local environment, which could influence the ARIS spectra. The influence of capillary waves on the results can be excluded since the maxima or minima of a wave cannot by nature be correlated with a certain specie in the outermost layer and thus cannot cause a lateral inhomogeneity in the local environment of an atom. A second possible influence could be the energy loss of the projectiles in the vapor above the surface. This influence becomes more important the smaller the angle of incidence is since the projectiles pass at grazing incidence more vapor than at a polar angle close to the surface normal. The energy loss in the vapor can be calculated from the trajectories of the projectiles assuming as upper limit for the vapor density the vapor pressure of the solvent. The maximum energy loss in

the vapor is for all angles about an order of magnitude smaller than the error bars shown in Fig. 9a.

Conclusion

We have shown that ARISS reveals the topography around atoms in a liquid surface. The topography is the average amount of matter around an atom in a certain direction which is given by the polar angle of the specific measurement. When comparing the topography around iodide and bromide we find that bromide is located in a deeper valley than iodide, which is explained with the difference in their ionic radii and solvation enthalpy. We find only a small difference between the topography around iodide for the solutes KI and Bu_4NI. The small difference is attributed to the different composition of the environment in the surface of both solutions, which consists in the first case mainly of the solvent formamide and in the latter case of the Bu_4N^+ cation.

Since the solvation energies of the investigated ions are similar for water and formamide,[30] the features of the topography determined with formamide as solvent could be similar to that of aqueous surfaces. Nevertheless, this has to be proven experimentally.

Acknowledgements

We thank Mr X. Gao who carried out some of the measurements shown here. This work has been sponsored by grants from the Deutsche Forschungsgemeinschaft (DFG; Mo 288/25).

References

1 L. X. Dang, *J. Phys. Chem. A*, 2004, **108**, 9014.
2 P. Jungwirth and D. J. Tobias, *J. Phys. Chem. B*, 2001, **105**, 10468.
3 J. Penfold, R. K. Thomas, J. R. Lu, E. Staples, I. Tucker and L. Thompson, *Physica B (Amsterdam)*, 1994, **198**, 110.
4 S. W. An, J. R. Lu, R. K. Thomas and J. Penfold, *Langmuir*, 1996, **12**, 2446.
5 Z. Zhang, D. M. Mitrinovic, S. M. Williams, Z. Huang and M. L. Schlossman, *J. Chem. Phys.*, 1999, **110**, 7421.
6 J. Penfold, *Rep. Prog. Phys.*, 2001, **64**, 777.
7 D. M. Mitrinovic, Z. Zhang, S. M. Williams, Z. Huang and M. L. Schlossman, *J. Phys. Chem. B*, 1999, **103**, 1779.
8 G. L. Richmond, *Chem. Rev.*, 2000, **102**, 2693.
9 X. Wei and Y. R. Shen, *Phys. Rev. Lett.*, 2001, **86**, 4799.
10 E. Hommel and H. Allen, *Analyst*, 2003, **128**, 750.
11 F. Eschen, M. Heyerhoff, H. Morgner and J. Vogt, *J. Phys.: Condens. Matter*, 1995, **7**, 1961.
12 O. A. Baschenko, F. Bökman, O. Bohman and H. O. G. Siegbahn, *J. Electron Spectrosc. Relat. Phenom.*, 1993, **62**, 317.
13 S. Baldelli, C. Schnitzer and M. J. Shultz, *J. Chem. Phys.*, 1998, **108**, 9817.
14 G. M. Nathanson, *Annu. Rev. Phys. Chem.*, 2004, **55**, 231.
15 G. Nathanson and A. Munter, to be published.
16 I. Watanabe, *J. Mol. Liq.*, 1995, **65/66**, 245.
17 G. Andersson and H. Morgner, *Surf. Sci.*, 2000, **445**, 89.
18 G. Andersson and H. Morgner, *Surf. Sci.*, 1998, **405**, 138.
19 G. Andersson, T. Krebs and H. Morgner, *Phys. Chem. Chem. Phys.*, 2005, **7**, 136.
20 M. Aono, M. Katayama, E. Nomura, T. Chassé, D. Choi and M. Kato, *Nucl. Instrum. Methods Phys. Res., Sect. B*, 1989, **37/38**, 264.
21 B. Moest, S. Helfensteyn, P. Deurinck, M. Nelis, A. W. Denier van der Gon, H. H. Brongersma, C. Creemers and B. E. Nieuwenhuys, *Surf. Sci.*, 2003, **536**, 177.
22 J. Dietter and H. Morgner, *Chem. Phys.*, 1999, **241**, 55.
23 H. Morgner, J. Oberbrodhage, K. Richter and K. Roth, *J. Phys.: Condens. Matter*, 1991, **3**, 5639.
24 J. Oberbrodhage, *J. Electron Spectrosc. Relat. Phenom.*, 1998, **95**, 171.
25 G. Andersson, *Phys. Chem. Chem. Phys.*, 2005, **7**, DOI: 10.1039/b504133c.
26 W. Keller, H. Morgner and W. A. Müller, *Mol. Phys.*, 1986, **57**, 623.
27 J. Oberbrodhage, H. Morgner, O. Tapia and H. O. G. Siegbahn, *Int. J. Quantum Chem.*, 1997, **63**, 1123.
28 G. Andersson, H. Morgner and K.-D. Schulze, *Nucl. Instrum. Methods Phys. Res., Sect. B*, 2002, **190**, 222.
29 O. Stern, *Z. Elektrochem.*, 1924, **30**, 508.
30 G. Somsen, *Recl. Trav. Chim. Pays-Bas*, 1966, **85**, 517.
31 K.-D. Schulze, G. Andersson and H. Morgner, in preparation.

